THE 200 AND 398 MEV ELASTIC SCATTERING OF PROTONS ON α-CLUSTER NUCLEI

YU.A. BEREZHNOY, V.P. MIKHAILYUK

Kharkov State University, Kharkov 310077, USSR*

AND

V.V. PILIPENKO

Institute of Physics and Technology, Kharkov 310108, USSR

(Received August 12, 1991)

The elastic scattering differential cross sections and polarization observables for 200 and 398 MeV protons on ^{12}C and ^{16}O nuclei are calculated on the basis of the multiple diffraction scattering theory and α-cluster model with dispersion. We have shown that our calculations and those based on the Kerman, McManus and Thaler theory lead to the systematic differences in the observables for p-^{12}C and p-^{16}O scattering at the energies considered.

PACS numbers: 24.10.Ht, 24.70.+s

1. Introduction

The α-cluster model is successfully used to describe the elastic scattering of protons and other particles on ^{12}C and ^{16}O nuclei [1–9]. The model in which the positions of α-clusters in ^{12}C and ^{16}O nuclei are fixed relative to each other was considered in Refs [1, 2]. In Ref. [3] it was supposed that the α-clusters in ^{12}C nucleus could be displaced from their most probable positions at the vertices of an equilateral triangle. But the model nuclear density of Ref. [3] was negative at small distances. In Refs [4, 5] the α-cluster model with dispersion was proposed in which the α-clusters could be displaced from their equilibrium positions at the vertices of an equilateral triangle (^{12}C nucleus) and tetrahedron (^{16}O nucleus). This model allowed

* Mailing address.

us to describe the differential cross sections and polarization observables for 500–1000 MeV proton elastic scattering on ^{12}C and ^{16}O nuclei and the differential cross sections of electron, pion and antiproton elastic scattering on these nuclei.

In Refs [6–9] on the basis of α-particle model, the optical potentials for proton and pion scattering on ^{12}C and ^{16}O nuclei were obtained from p-α and π-α amplitudes. This optical model describes the differential cross sections and polarization observables for 200–400 MeV proton elastic scattering on carbon and oxygen nuclei [8,9]. The agreement between the quantities calculated in Refs [8,9] and the measured ones is surprising since, as it seems to us, the construction of the optical potential for the system of three and four particles is insufficiently well founded.

Thus, the α-cluster model with dispersion allows us to describe the observables in proton elastic scattering on ^{12}C and ^{16}O nuclei in a wide energy region. This approach is attractive as the α-cluster model takes into account the correlations between the nucleons of the α-clusters and the correlations between the α-clusters. Since the α-particle has a zero spin the p-α amplitude consists of two terms — central and spin-orbit parts which are actually averaged over the spins of the nucleons in the α-particle.

The success of the α-cluster model with dispersion [4, 5] in describing the elastic scattering of 500–1000 MeV protons allows us to suppose that this model should describe the observables in 200–400 MeV proton scattering on carbon and oxygen nuclei. For this reason we have carried out the theoretical analysis of the measured differential cross sections, polarizations (asymmetries) and spin-rotation functions for 200 and 398 MeV proton scattering on ^{12}C and ^{16}O nuclei.

In Section 2 the α-cluster model with dispersion is discussed and the densities of the α-particle distribution in ^{12}C and ^{16}O nuclei are given.

Section 3 gives the parametrization of the p-α amplitude which allows us to approximate the experimental data on the p-^{4}He elastic scattering in the range of the transferred momenta $-t \lesssim 0.7$ (GeV/c)^2. Here we also present the expressions for the p-^{12}C and p-^{16}O scattering amplitudes calculated on the basis of the α-cluster model with dispersion [4, 5] in the effective deformation approximation [2].

In Section 4 we make a comparison between the calculated and measured observables for p-^{12}C and p-^{16}O elastic scattering. The analysis made shows that the agreement between the calculated and measured quantities is better for the scattering of 398 MeV than of 200 MeV protons. It may be due to the fact that the validity conditions of the multiple diffraction scattering theory (MDST) [10, 11] used by us for proton interaction with three- and four-α-particle systems making up ^{12}C and ^{16}O nuclei are fulfilled better for higher energies.

2. The α-cluster model with dispersion

In the first approximation the ^{12}C and ^{16}O nuclei can be considered as composed of α-particles which are fixed relative to each other at vertices of an equilateral triangle (^{12}C nucleus) and tetrahedron (^{16}O nucleus) [1]. In this case the densities of the α-particle distribution are determined by

$$\rho_0^{(C)}(\vec{\xi},\vec{\eta}) = \frac{1}{4\sqrt{3}\pi^2 d^2}\delta(\xi - d)\delta(\eta - \tfrac{\sqrt{3}}{2}d)\delta(\vec{\xi}\vec{\eta}), \tag{1}$$

$$\rho_0^{(O)}(\vec{\xi},\vec{\eta},\vec{\zeta}) = \frac{1}{(4\pi)^2}\delta(\xi - d)\delta(\eta - \tfrac{\sqrt{3}}{2}d)\delta(\xi - \sqrt{\tfrac{2}{3}}d)\delta(\vec{\xi}\vec{\eta})\delta(\vec{\xi}\vec{\zeta})\delta(\vec{\eta}\vec{\zeta}), \tag{2}$$

where d is the distance between two α-particles, and the Jacobi coordinates are related to the α-particle coordinates through

$$\vec{\xi} = \vec{r}_2 - \vec{r}_1, \quad \vec{\eta} = \vec{r}_3 - \tfrac{1}{2}(\vec{r}_1 + \vec{r}_2), \quad \vec{\zeta} = \vec{r}_4 - \tfrac{1}{3}(\vec{r}_1 + \vec{r}_2 + \vec{r}_3). \tag{3}$$

According to the α-cluster model with dispersion [4, 5] the ^{12}C and ^{16}O densities are determined by

$$\rho_\Delta^{(C)}(\vec{\xi},\vec{\eta}) = \int d^3\xi' d^3\eta' \rho_0^{(C)}(\vec{\xi}',\vec{\eta}')\Phi_\Delta^{(C)}(\vec{\xi} - \vec{\xi}', \vec{\eta} - \vec{\eta}'). \tag{4}$$

$$\rho_\Delta^{(O)}(\vec{\xi},\vec{\eta},\vec{\zeta}) = \int d^3\xi' d^3\eta' d^3\zeta' \rho_0^{(O)}(\vec{\xi}',\vec{\eta}',\vec{\zeta}')\Phi_\Delta^{(O)}(\vec{\xi}-\vec{\xi}', \vec{\eta}-\vec{\eta}', \vec{\zeta}-\vec{\zeta}'). \tag{5}$$

The smearing functions $\Phi_\Delta^{(C)}(\vec{\xi},\vec{\eta})$ and $\Phi_\Delta^{(O)}(\vec{\xi},\vec{\eta},\vec{\zeta})$ can be chosen in the Gaussian forms

$$\Phi_\Delta^{(C)}(\vec{\xi},\vec{\eta}) = \frac{1}{(\sqrt{3}\pi\Delta^2)^3}\exp\Big(-\frac{\xi^2 + (4/3)\eta^2}{2\Delta^2}\Big), \tag{6}$$

$$\Phi_\Delta^{(O)}(\vec{\xi},\vec{\eta},\vec{\zeta}) = \frac{1}{8(\pi\Delta)^9}\exp\Big(-\frac{\xi^2 + (4/3)\eta^2 + (3/2)\zeta^2}{2\Delta^2}\Big), \tag{7}$$

where the dispersion parameter Δ characterizes the probability of the α-particle displacement from its most probable position at the vertices of the equilateral triangle (^{12}C nucleus) or tetrahedron (^{16}O nucleus). It can be easily seen that the smearing functions $\Phi_\Delta^{(C)}(\vec{\xi},\vec{\eta})$ and $\Phi_\Delta^{(O)}(\vec{\xi}\vec{\eta},\vec{\zeta})$ are transformed into $\delta(\vec{\xi})\,\delta(\vec{\eta})$ and $\delta(\vec{\xi})\,\delta(\vec{\eta})\,\delta(\vec{\zeta})$ respectively, if $\Delta = 0$.

The densities $\rho_{\Delta}^{(C)}(\vec{\xi},\vec{\eta})$ and $\rho_{\Delta}^{(O)}(\vec{\xi},\vec{\eta},\vec{\zeta})$ are invariant under the rearrangement of any pair of α-particles. This means an invariance to transformations

$$\vec{\xi} \to -\vec{\xi}, \tag{8}$$

$$\vec{\xi} \to \tfrac{1}{2}\vec{\xi} - \vec{\eta}, \quad \vec{\eta} \to -\tfrac{3}{4}\vec{\xi} - \tfrac{1}{2}\vec{\eta}, \tag{9}$$

$$\vec{\xi} \to \tfrac{1}{2}\vec{\xi} - \tfrac{1}{3}\vec{\eta} - \vec{\zeta}, \quad \vec{\eta} \to -\tfrac{1}{4}\vec{\xi} + \tfrac{5}{6}\vec{\eta} - \tfrac{1}{2}\vec{\zeta}, \quad \vec{\zeta} \to -\tfrac{2}{3}\vec{\xi} - \tfrac{4}{9}\vec{\eta} - \tfrac{1}{3}\vec{\zeta}. \tag{10}$$

The parameters of the densities $\rho_{\Delta}^{(C)}(\vec{\xi},\vec{\eta})$ and $\rho_{\Delta}^{(O)}(\vec{\xi},\vec{\eta},\vec{\zeta})$ can be determined from the comparison of the calculated and measured charge formfactors of ^{12}C and ^{16}O nuclei. The formfactors of ^{12}C and ^{16}O nuclei as of systems of three and four α-particles can be written as

$$F_{(q)}^{(C)} = F_{\alpha}(q) \int d^3\xi d^3\eta \exp\left(\tfrac{2}{3} i\vec{q}\vec{\eta}\right) \rho_{\Delta}^{(C)}(\vec{\xi},\vec{\eta}), \tag{11}$$

$$F^{(O)}(q) = F_{\alpha}(q) \int d^3\xi d^3\eta d^3\zeta \exp\left(\tfrac{3}{4} i\vec{q}\vec{\zeta}\right) \rho_{\Delta}^{(O)}(\vec{\xi},\vec{\eta},\vec{\zeta}), \tag{12}$$

where q is the transferred momentum, $F_{\alpha}(q)$ is the α-particle formfactor which can be taken in the Gaussian form [12]

$$F_{\alpha}(q) = \exp\left(-\tfrac{1}{6} q^2 \langle r^2\rangle_{\alpha}\right). \tag{13}$$

Here $\langle r^2\rangle_{\alpha}^{1/2} = 1.61$ fm is RMS radius of the α-particle.

Integrating in equations (11) and (12) yields

$$F^{(C)}(q) = F_{\alpha}(q) j_0\left(\frac{qd}{\sqrt{3}}\right) \exp\left(-\tfrac{1}{6} q^2 \Delta^2\right), \tag{14}$$

$$F^{(O)}(q) = F_{\alpha}(q) j_0\left(\sqrt{\frac{3}{8}} qd\right) \exp\left(-\tfrac{3}{16} q^2 \Delta^2\right). \tag{15}$$

The parameters d and Δ were determined in Refs [4, 5]: $d = 2.98$ fm, $\Delta = 0.346$ fm for the ^{12}C nucleus and $d = 3.16$ fm, $\Delta = 0.643$ fm for the ^{16}O nucleus. As is shown in Refs [4, 5], these values of the parameters d and Δ allow us to describe the measured formfactors of ^{12}C and ^{16}O nuclei up to the values of the transferred momenta $q \lesssim 3$ fm^{-1}.

It is seen from equations (14) and (15) that the introduction of the smearing functions $\Phi_{\Delta}^{(C)}(\vec{\xi},\vec{\eta})$ and $\Phi_{\Delta}^{(O)}(\vec{\xi},\vec{\eta},\vec{\zeta})$ into the densities (4) and (5) results in the occurrence of additional exponential factors in the formfactors, which do not change their qualitative behaviour and lead to a more rapid decrease with the increase of the transferred momentum.

3. The scattering amplitude of protons on carbon and oxygen nuclei

Consider the interaction of intermediate energy protons with ^{12}C and ^{16}O nuclei. We assume that the interaction of the incident protons with α-particles constituting ^{12}C and ^{16}O nuclei is the same as that with free α-particles, so that we can use the MDST [10, 11]. Then the scattering amplitude of protons on ^4He nuclei can be written as

$$f_{p\alpha}(\vec{q}) = f_c(q) + f_s(q)\vec{\sigma}\vec{n}, \tag{16}$$

where $\vec{\sigma}$ is the spin operator of the incident proton, $\vec{n} = [\vec{k}, \vec{k}']/|[\vec{k}, \vec{k}']|$, $\vec{k}$ and $\vec{k}'$ are the wavevectors of the incident and scattered proton.

To determine the central $f_c(q)$ and spin-orbit $f_s(q)$ parts of the p-^{4}He elastic scattering amplitude, we proposed the following parametrization [5]

$$f_c(q) = k\Big(G_1 \exp\left(-\beta_1 q^2\right) + G_2 \exp\left(-\beta_2 q^2\right)\Big), \tag{17}$$

$$f_s(q) = kq\Big(G_3 \exp\left(-\beta_3 q^2\right) + G_4 \exp\left(-\beta_4 q^2\right)\Big). \tag{18}$$

In equations (17) and (18) the complex parameters G_1, G_3, β_1 and β_3 are determined by fitting the differential cross sections and polarization observables of protons elastically scattered on ^{4}He nuclei, and the parameters G_2, G_4, β_2 and β_4 are related to G_1, G_3, β_1 and β_3 by

$$G_2 = \frac{3iG_1^2}{32\beta_1}, \qquad G_4 = \frac{3iG_1G_3\beta_1}{8(\beta_1+\beta_3)^2},$$
$$\beta_2 = \tfrac{1}{2}\beta_1, \qquad \beta_4 = \frac{\beta_1\beta_3}{\beta_1+\beta_3}. \tag{19}$$

The relations (19) between the parameters are chosen so that the terms with G_2 and G_4 in (17) and (18) correspond to the leading terms coming from the double proton-nucleon scattering when the p-α amplitude is calculated in the MDST with the Gaussian single-particle density of the ^{4}He nucleus. We should, however, emphasize that the amplitude (16)–(18) cannot be considered as the calculated by the MDST. This amplitude is a phenomenological one and is used to approximate the experimental data on the p-^{4}He scattering. By making use of this p-α amplitude parameterization the experimental data for elastic p-^{4}He scattering at the energies $E \gtrsim 500$ MeV were fitted [5].

Notice that in Refs [4, 13] $f_c(q)$ and $f_s(q)$ are taken in the form of one Gaussian function ($G_2 = G_4 = 0$). But this choice of the p-α amplitude allows one to fit the observables in elastic p-^{4}He scattering only in the region of small transferred momenta.

In Refs [8, 9] a different parameterization of $f_c(q)$ and $f_s(q)$ was proposed

$$f_c(q) = k\widetilde{G}_1(1-\tau_1 q^2)(1-\tau_2 q^2)\exp\left(-\beta_c q^2\right), \tag{20}$$

$$f_s(q) = kq\widetilde{G}_3(1-\tau_3 q^2)(1-\tau_4 q^2)\exp\left(-\beta_s q^2\right). \tag{21}$$

To calculate the p-^{12}C and p-^{16}O elastic scattering amplitudes we need the numerical values of the parameters of the p-α amplitude. For this reason we carried out the fitting of the measured differential cross section $\sigma \equiv d\sigma/dt$ and polarization P for elastic p-^{4}He scattering at 200 and 350 MeV energies [14] (Figs 1 and 2). The parameters obtained from this comparison of observables are presented in the Table. Notice that some discrepancies in the calculated and measured observables in the region of small transferred momenta can be associated with the fact that our parametrization of p-α amplitude does not take into account the Coulomb interaction.

TABLE

E [MeV]	β_1 [fm^2]	β_3 [fm^2]	G_1 [fm^2]	G_3 [fm^3]
200	$0.295 - 0.283$	$0.937 + 0.430$	$0.213 + 0.726$	$-0.293 + 0.563$
350	$0.309 - 0.116$	$0.498 + 0.098$	$-0.092 + 0.857$	$0.206 + 0.397$
398	$0.375 - 0.085$	$0.492 - 0.095$	$-0.184 + 0.914$	$0.202 + 0.402$

To determine the parameters of p-α amplitude more precisely it is necessary to know three independent observables. But the experimental data for the third observable (Wolfenstein parameter R, spin-orbit function Q *etc.*) in elastic p-^{4}He scattering at 200 and 350 MeV energies is not available. We have calculated the values of R for the p-α amplitude in the form (17), (18) (Figs 1 and 2, solid curves) with the parameters presented in the Table and for the p-α amplitude in the form (20),(21) (Figs 1 and 2, dashed curves) with the parameters taken from Refs [8, 9]. The results of the calculations show that the behaviour of R is very sensitive to the choice of the parameters of p-α amplitude. It should be emphasized that the qualitative behaviour of the Wolfenstein parameter is in agreement with the values of R calculated [5] and measured [15] at 500 MeV energy.

Notice that to reach the agreement between the calculated and measured observables at 200 MeV we need to consider the parameters G_2 and G_4 as the fitting ones. At the same time the parameters β_2, β_4 and β_1, β_3 are related through equations (19). We have obtained the following values of the parameters G_2 and G_4 : $G_2 = (0.090 - i\,0.183)$ fm^2,

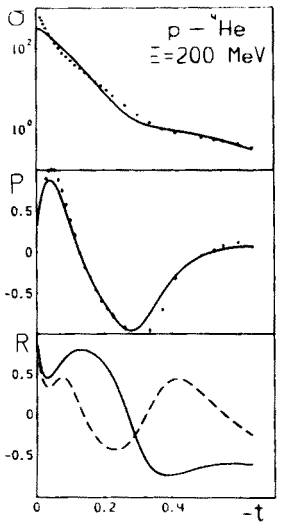

Fig. 1

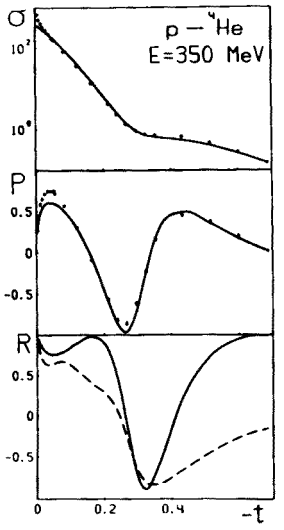

Fig. 2

Fig. 1. Elastic scattering differential cross section (mb/(GeV/c)^2), polarization P and Wolfenstein parameter R for 200 MeV protons scattered on ^{4}He as functions of the square 4-momentum transferred $-t((\mathrm{GeV}/c)^2)$. The solid curves are calculated with p-α amplitude in the form (17), (18) and dashed curve is calculated with the p-α amplitude in the form (20, (21). Experimental data are taken from [14].

Fig. 2. The same as in Fig. 1, for p-^{4}He at 350 MeV. Experimental data taken from [14].

$G_4 = (0.130 - i\,0.025)\mathrm{fm}^3$. The parameters of p-$\alpha$ amplitude at 398 MeV energy presented in the Table are obtained by interpolating these values at 350 and 500 MeV [5]. This choice of the parameters of p-α amplitude at the 398 MeV energy is due to the lack of the experimental data on p-^{4}He scattering for this energy.

According to MDST [10,11] the p-^{12}C and p-^{16}O elastic scattering amplitudes are given as

$$F^{(\mathrm{C})}(\vec{q}) = \frac{ik}{2\pi}\int d^2b\,d^3\xi\,d^3\eta\,\rho_{\Delta}^{(\mathrm{C})}(\vec{\xi},\vec{\eta})\exp\left(i\vec{q}\vec{b}\right)$$

$$\times\left(1-\prod_{j=1}^{3}\left(1-\frac{1}{2\pi ik}\int f_{p\alpha}(\vec{q}')\exp\left(-i\vec{q}'(\vec{b}-\vec{r}_j)\right)d^2q'\right)\right), \qquad (22)$$

$$F^{(\mathrm{O})}(\vec{q}) = \frac{ik}{2\pi}\int d^2b\,d^3\xi\,d^3\eta\,d^3\zeta\,\rho_{\Delta}^{(\mathrm{O})}(\vec{\xi},\vec{\eta},\vec{\zeta})\exp\left(i\vec{q}\vec{b}\right)$$

$$\times\left(1-\prod_{j=1}^{4}\left(1-\frac{1}{2\pi ik}\int f_{p\alpha}(\vec{q}')\exp\left(-i\vec{q}'(\vec{b}-\vec{r}_j)\right)d^2q'\right)\right), \qquad (23)$$

where $\vec{b}$ is the impact parameter which lies in the plane perpendicular to the incident beam. The explicit expressions for the amplitudes $F^{(C)}(q)$ and $F^{(O)}(q)$ are presented in [5].

Notice that to calculate the integrals in formulae (22), (23) we use the effective deformation approximation [2]. As it was shown in Ref. [4], this approach yields the results which do not significantly differ from those calculated by the exact formulae, and allows us to obtain the p-^{12}C and p-^{16}O elastic scattering amplitudes in the closed form.

4. Comparison with the experimental data

On the basis of the above approach we calculated the differential cross sections $\sigma \equiv d\sigma/d\Omega$, polarizations P and spin-rotation functions Q for elastic p-^{12}C scattering at 200 and 398 MeV and p-^{16}O scattering at 200 MeV. The results of these calculations along with the experimental data from Refs [16, 17] are presented in Figs 3–8. Figs 3, 5 and 7 show the observables calculated with the p-α amplitude which was taken in the form (17), (18) and Figs 4,6 and 8 (solid curves) show these calculated with the p-α amplitude in the form (20, (21) with the set of parameters given in Refs [8,9].

In the calculations of the observables with the amplitudes (22, (23) in which the p-α amplitude was taken in the form (20), (21 (Figs 4, 6 and 8, solid curves) the single scattering amplitudes were calculated exactly. The amplitudes of higher scattering multiplicity were calculated by using the following approximation [5]

$$f_c(q) = k\tilde{G}_1 \exp\left(-\tilde{\beta}_1 q^2\right), \tag{24}$$

$$f_s(q) = kq\tilde{G}_3 \exp\left(-\tilde{\beta}_3 q^2\right), \tag{25}$$

where $\tilde{\beta}_1 = \beta_c + \tau_1 + \tau_2$ and $\tilde{\beta}_3 = \beta_s + \tau_3 + \tau_4$. This approximation is valid in the region of small transferred momenta q.

In Figs 4, 6 and 8 the observables calculated in Refs [8,9] (dashed curves) are also shown. In these papers the differential cross sections, polarizations P and spin-rotation functions Q for elastic p-^{12}C and p-^{16}O scattering were calculated on the basis of the optical model. The complex potential of the model was constructed in the framework of the Kerman, McManus and Thaler (KMT) theory [18] by using the single-particle distribution and p-α amplitudes which were taken in the form (20), (21).

Figures 3 and 5 show that the results of the calculations performed on the basis of MDST with p-α amplitude in the form (17), (18) and by using the α-cluster model with dispersion correctly describe the behaviour of the

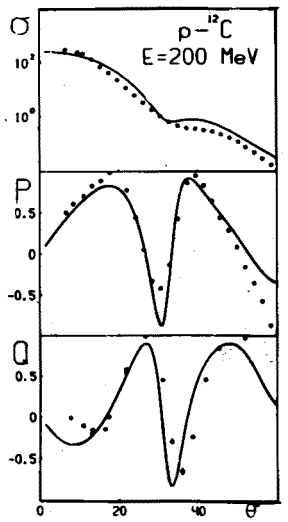

Fig. 3

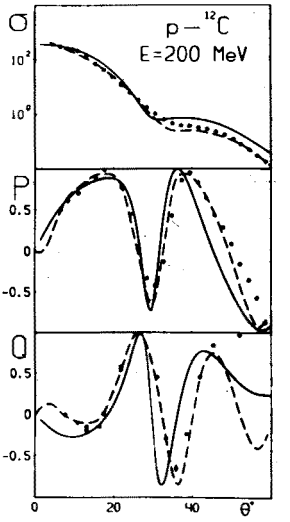

Fig. 4

Fig. 3. Elastic scattering differential cross section $\sigma(\theta)$ (mb/sr), polarization $P(\theta)$ and spin-rotation function $Q(\theta)$ for p-^{12}C at 200 MeV. The curves are calculated with p-α amplitude in the form (17), (18). Experimental data are taken from [16].

Fig. 4. The same as in Fig. 3. The solid curves are calculated with p-α amplitude in the form (20, (21) and the dashed curves are taken from [8].

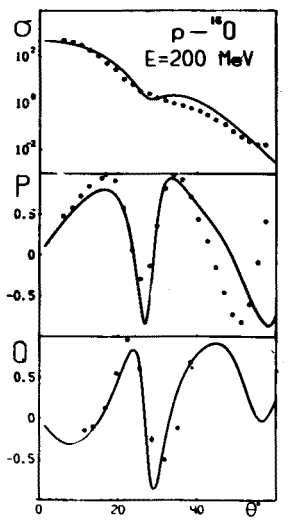

Fig. 5

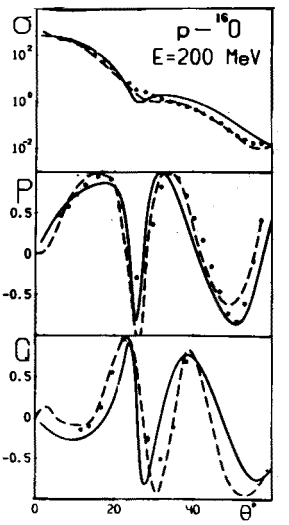

Fig. 6

Fig. 5. The same as in Fig. 3, for p-^{16}O.

Fig. 6. The same as in Fig. 4 for p-^{16}O.

observables in elastic p-^{12}C and p-^{16}O scattering at 200 MeV. However, it should be noticed that in the region of large scattering angles the calculated differential cross sections exceed the measured ones. The same difference is observed in the behaviour of the differential cross section calculated on the basis of MDST with the p-α amplitude in the form (20), (21) (see Figs 4 and 6). Though, the behaviour of the differential cross section is similar, the polarization observables calculated with different p-α amplitudes differ significantly. It is not surprising because the p-α amplitudes taken in the form (17), (18) or (20), (21) lead to a different behaviour of the p-^{4}He Wolfenstein parameter R. In our calculations the best agreement between the calculated and measured observables for elastic p-^{12}C and p-^{16}O scattering is observed in the case of the p-α amplitude in the form (17) and (18). It should be recognized, however, that the p-α amplitude in this case is determined insufficiently reliable because of the lack of the data on third independent observable for p-^{4}He elastic scattering. Notice also that the validity conditions of MDST, in particular the requirement of rapid falloff of p-α amplitude with the increase of the momentum transferred are fulfilled insufficiently well for 200 MeV proton energy. The results of the calculations performed in Ref. [8] on the basis of the optical potential which was obtained from the α-cluster model with p-α amplitude (20), (21) differ significantly from the results we obtained on the basis of MDST with the same p-α amplitude.

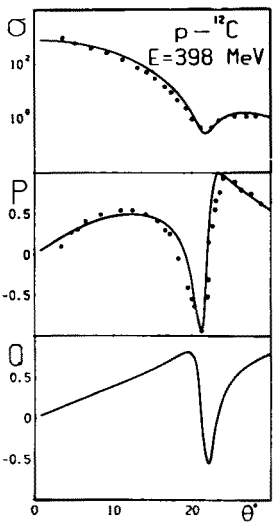

Fig. 7

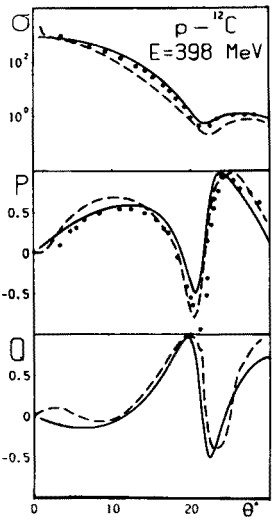

Fig. 8

Fig. 7. The same as in Fig. 3, for p-^{12}C at 398 MeV. Experimental data are taken from [17].

Fig. 8. The same as in Fig. 4, for p-^{12}C at 398 MeV.

As can be seen from Fig. 7, the α-cluster model with dispersion and MDST with p-α amplitude in the form (17), (18) provide a good description of the differential cross section and polarization for elastic p-^{12}C scattering at 398 MeV. Similar calculations with p-α amplitude taken in the form (20), (21) give an equally well describe the polarization as in Fig. 8. Notice that the behaviour of the spin rotation functions Q, for which the experimental data are not available, differs for these two p-α amplitudes even qualitatively. The behaviour of the function Q shown in Fig. 7 is similar to the one for p-^{12}C and p-^{16}O scattering at higher energies (see Ref. [5]). Notice that the validity conditions of MDST are fulfilled better for 398 MeV than for 200 MeV. If the same p-α amplitude (in the form (20) and (21)) is used, then the results of the calculations by our model and those made by the model of Ref. [8] differ in the same way from each other (see Fig. 8) as it was observed at 200 MeV.

5. Conclusions

In this work the theoretical calculations of differential cross sections and polarization observables for elastic p-^{12}C and p-^{16}O scattering at 200 and 398 MeV were made. The calculations were performed on the basis of MDST in which the p-^{12}C and p-^{16}O amplitudes were constructed by using the p-α amplitudes and many particle densities of the α-particle distribution in ^{12}C and ^{16}O nuclei. These densities chosen in accordance with the α-cluster model with dispersion. We have used two different parametrizations of p-α amplitude. Their parameters were determined from the p-^{4}He scattering data. It has been shown that the model proposed allows us to describe correctly the measured observables for elastic p-^{12}C and p-^{16}O scattering at energies considered. The agreement between the calculated and measured quantities is better for 398 MeV protons when the validity conditions of MDST are fulfilled better. We have shown that the spin-rotation functions Q of protons elastically scattered on ^{12}C and ^{16}O nuclei is very sensitive to the choice of the form of the p-α amplitude. In the calculations with two different parametrizations of the p-α amplitude for 398 MeV protons the qualitative distinctions in the behaviour of the function Q are obvious. At the same time the difference in the calculated differential cross sections and polarizations in this case is very slight.

Notice that the calculations performed in this work and those taken from Refs [8, 9] *i.e.*the calculations based on the KMT theory, lead to the systematic differences in the behaviour of the observables for carbon and oxygen nuclei at both energies considered if the same parametrization of p-α amplitude is used.

We thank D.M. Skrypnik for assistance in preparing the English version of this paper.

REFERENCES

[1] E.V. Inopin, B.I. Tishchenko, *Zh. Eksp. Teor. Fiz.* **11**, 840 (1960).
[2] I. Ahmad, *Phys. Lett.* **36B**, 301 (1975).
[3] G.F. Germond, C.W. Wilkin, *Nucl. Phys.* **A237**, 477 (1975).
[4] Yu.A. Berezhnoy, V.V. Pilipenko, G.A. Khomenko, *J. Phys. G* **10**, 63 (1984).
[5] Yu.A. Berezhnoy, V.P. Mikhailyuk, V.V. Pilipenko, *Acta Phys. Pol.* **B21**, 723 (1990).
[6] Li Qing-Run, *Nucl. Phys.* **A415**, 445 (1984).
[7] Li Qing-Run, *Phys. Rev.* **C30**, 1248 (1984).
[8] Z.Q. Tan, W.Y. Ruan, *J. Phys. G* **15**, 1599 (1989).
[9] Z.Q. Tan, W.Y. Ruan, *Nucl. Phys.* **A514**, 295 (1990).
[10] R.J. Glauber, *Lectures in Theoretical Physics*, Vol. 1, Eds. W.E. Brittin, L.G. Dunham, Interscience, New York 1959 p. 315.
[11] A.G. Sitenko, *Ukr. Fiz. Zh.* **4**, 152 (1959).
[12] R. Hofstadter, *Rev. Mod. Phys.* **28**, 214 (1956).
[13] I. Ahmad, Z.A. Khan, *Nucl. Phys.* **A274**, 519 (1976).
[14] G.A. Mose *et al.*, *Phys. Rev.* **C21**, 1932 (1980).
[15] G.A. Mose *et al.*, *Nucl. Phys.* **A392**, 361 (1988).
[16] D.P. Murdock, C.J. Horowitz, *Phys. Rev.* **C35**, 1442 (1987).
[17] G.S. Adams *et al. Phys. Rev. Lett.* **43**, 421 (1979).
[18] A.K. Kerman, H. McManus, R.H. Thaler, *Ann. Phys.* **8**, 551 (1959).